

A Comparative DFT Study on Structural and Electronic Properties of C₂₄ and Some of Its Derivatives: C₁₂B₆N₆, B₆N₆C₁₂ and B₁₂N₁₂

M. Anafche and F. Naderi*

¹Department of Chemistry, Shahr-e-Qods Branch, Islamic Azad University, Tehran, Iran

Received March 2012; Accepted April 2012

ABSTRACT

The structural stabilities, geometry and electronic properties of C₂₄ and some its heterofullerene derivatives are compared at the B3LYP/6-311++G**//B3LYP/6-31+G* level of theory. Vibrational frequency calculations show that all the systems are true minima. The calculated binding energies of heterofullerenes show C₂₄ as the most stable fullerenes by 9.03eV/atom. While decreasing binding energy in C₁₂B₆N₆, B₆N₆C₁₂ and B₁₂N₁₂ through increasing their HOMO-LUMO gap, the conductivity of them is increasing. High point charges are predicted to establish an overall charge transfer on the surface of heterofullerene. ¹³C NMR of C₂₄ fullerene consists of two lines. Doped models show several lines at different positions relative to lines for C₂₄ fullerene. Boron, nitrogen, and carbon adopt different roles around carbon sites. The Nucleus-independent chemical shift (NICS) calculations show more negative NICS values in BN-substituted heterofullerenes than those of C₂₄.

Keywords: Heterofullerene; Substitutional doping; NBO analysis; NICS; DFT

INTRODUCTION

Fullerenes are accepted as the fourth form of solid carbon after amorphous, graphite and diamond forms. Indeed, fullerene materials provide different doping possibilities, including substitutional doping, endohedral doping, and exohedral doping [1]. The discovery of C₆₀ [2,3] has attracted increasing attention toward similar types of cage structured compounds resulted from different doping strategies.

Larger fullerenes C_n (n = 20, 24, 28, 32, 36, and 40) with mono-BN-replacement are theoretically investigated [4]. For even larger clusters, Chen et al. studied the BN-substituted fullerenes C_{60-2x}(BN)_x and C_{70-2x}(BN)_x (x = 1-3) [5,6].

We focus our calculations on C₂₄ and some of its derivatives which are the isoelectronic analogues to carbon fullerenes. We compare and contrast these fullerenes both from the stability and application viewpoints. We are pleased to report that most of our devised heterofullerenes may serve as hydrogen carriers because of their high point charges. So, this has motivated the synthesis of alloys composed of these materials. Furthermore It is interesting to note that the simple cubic fullerite C₂₄ (or B₁₂N₁₂) has a two dimensional lattice of cylindrical nanopores with a diameter of 0.41 nm, and, hence, may find its application as molecular sieves [7].

* Corresponding author: fnaderi2@yahoo.com

COMPUTATIONAL METHOD

Full geometry optimizations are accomplished by means of hybrid functional B3LYP [8-10] and the 6-31+G* basis set, as implemented in Gaussian 98 [11]. The applied basis set is comprised of Pople's well known 6-31G* basis set [12,13] and an extra plus due to the importance of diffuse functions [14,15]. Vibrational frequency computations confirm that the fully optimized structures are indeed minima (NIMAG = 0). As a stability criterion of different configurations, binding energies are calculated according to the following expression:

$$E_b = pE_C + qE_B + rE_N - E \quad (1)$$

Where E is the total energy of the fullerene, p, q and r are the number of carbon, boron and nitrogen respectively. Systems with larger binding energies are more stable. Magnetic shielding and nuclear independent chemical shifts (NICSS) were also evaluated using the gauge-independent atomic orbital (GIAO) method with the 6-31+G* basis set. The CS tensors at the sites of ^{13}C nuclei are calculated [16]. The calculated CS tensors in principal axes system (PAS) ($\sigma_{33} > \sigma_{22} > \sigma_{11}$) are converted to measurable NMR parameters, chemical shielding isotropic (σ_{iso}) using (1) [17], respectively.

$$\sigma_{\text{iso}} (\text{ppm}) = 1/3(\sigma_{11} + \sigma_{22} + \sigma_{33}) \quad (2)$$

The chemical shielding tensor, σ , describes the electronic effect on the Zeeman energy levels of magnetic nuclei, due to the response of the electrons to a static external magnetic field, B_0 [18].

Natural bonding orbital (NBO) analysis [19] were performed on wave functions calculated at the B3LYP/6-31G* level of theory, as a standard program option in Gaussian 98.

RESULTS AND DISCUSSION

The optimized structures of parent cages (carbon C_{24} and boron nitride $\text{B}_{12}\text{N}_{12}$

fullerene) are shown in Fig. 1. Also the substitution of six CC units in C_{24} carbon fullerene which result to $\text{C}_{12}\text{B}_6\text{N}_6$, and the substitution of six BN units in $\text{B}_{12}\text{N}_{12}$ nanocage which result to $\text{B}_6\text{N}_6\text{C}_{12}$ are shown in Fig.1.

Geometry optimizations and resulted binding energies

The optimized geometries of the stable C_{24} and some of its analogs (Fig. 1) in the gas phase are listed in Table 1.

The C-C bond lengths of C_{24} are 1.423 Å, which is pretty close to the sum of covalent radii of two C atoms (C: 0.76 Å). Similarly, the C-B and C-N bond lengths of $\text{C}_{12}\text{B}_6\text{N}_6$ and $\text{B}_6\text{N}_6\text{C}_{12}$ systems are quite close to the sum of covalent radii of C and B or N atoms. The covalent radii of atoms are about 0.84 and 0.71 Å for B and N respectively.

The C_{24} (D_6) structure is the most stable one [20]. This fullerenic structure can be regarded as a 12 trannulene [21] capped with two benzene rings at both sides. The pentagonal faces share edges with one another but are held together by two hexagons. The stability of this shell should be higher than the stability of fullerene C_{20} (binding energy=6.06 eV/atom), in which all 12 pentagons are in contact with each other.

Its optimized structure is indeed affirmative of such a consideration with the uniform C-C bond length (1.423 Å) of the benzene-like rings, the localized C=C bond lengths of 1.365 Å and C-C bond lengths of 1.462 Å in the central 12 trannulenic ring, and the much longer C-C bond lengths of 1.531 Å between the six- membered rings and the central 12 trannulenic ring. These values are in an excellent agreement with [22].

$\text{C}_{12}\text{B}_6\text{N}_6$ consists of 12 pentagons and two hexagons (Fig. 1). The shell lacks the center of symmetry; therefore, the symmetry is reduced to C_1 . The pentagonal faces share edges with one another but are held together by two hexagons.

$\text{B}_6\text{N}_6\text{C}_{12}$ is formed from eight 6-membered rings and six 4-membered rings with C_1

symmetry. $B_{12}N_{12}$ is formed from eight 6-membered rings and six 4-membered rings with T_h symmetry so that the calculated electric dipole moment is zero. There are two distinct B-N bonds in the optimized structures of $B_{12}N_{12}$. One is shared by two 6-membered rings and another by 4- and 6-membered rings where length of this later (1.486 Å) is greater than that the former (1.439 Å). In these three later structures, all B-N bonds are shorter than the single bond in H_2B-NH_2 (1.674 Å) but

longer than the double bond in $HB=NH$ (1.391 Å).

Binding energy per atom, a criterion of stability, is calculated to be 9.03 eV/atom for C_{24} at B3LYP/6-31+G* (Table 2). Substituting C atoms with B and N reduces this value which is the result of the weakness of X-C bond vs. C-C bond. The calculated binding energy for $C_{12}B_6N_6$, $B_6N_6C_{12}$ and $B_{12}N_{12}$ are 8.69 to 8.63 eV/atom as you see in table 3 less than that of C_{24} with equivalent C-C bonds. It is approximately in accord

Table 1. Point groups (PG), total energies (E_{tot} in a.u.), ranges of carbon-carbon, N-C, B-C and B-N bond lengths (Å) at the B3LYP/6-31+G* level

Species	PG	E_{tot}	C-C	C=C	C-B	C-N	B-N
C_{24}	D_6	-913.86582	1.423-1.462	1.365	-	-	-
$C_{12}B_6N_6$	C_i	-934.89035	1.480	1.375	1.543-1.611	1.418-1.463	1.473-1.483
$B_6N_6C_{12}$	C_s	-934.89665	1.463-1.488	1.366	1.552	1.376-1.471	1.431-1.498
$B_{12}N_{12}$	T_h	-956.16544	-	-	-	-	1.439 -1.486

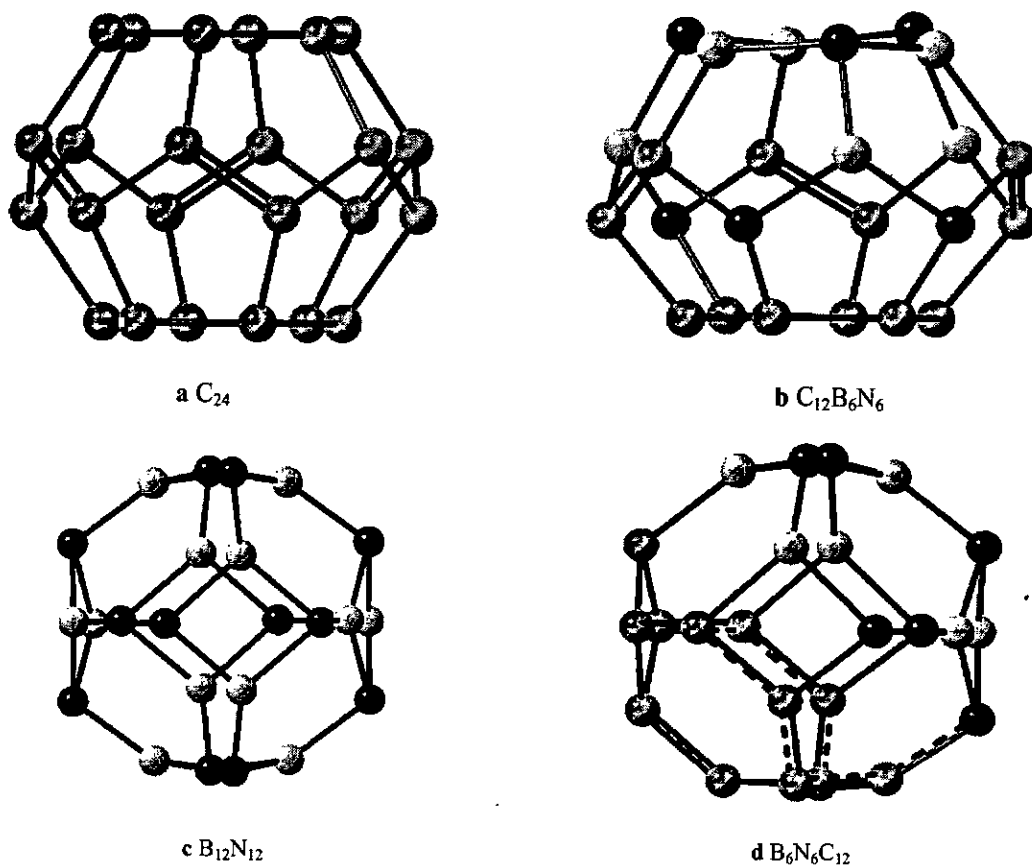


Fig. 1. Optimized heterofullerenes at B3LYP/6-31+G.

Table 2. Binding energies (B.E.) at B3LYP/6-31+G* and, the number of imaginary frequency and NICS values

Species	Binding Energy (eV/atom)	NIMAG	NICS (cage)
C ₂₄	9.03	0	36.51
C ₁₂ B ₆ N ₆	8.69	0	-10.93
B ₆ N ₆ C ₁₂	8.69	0	-0.67
B ₁₂ N ₁₂	8.63	0	-1.51

Table 3. Ranges of NBO atomic charges of carbon (C) and heteroatom for heterofullerenes at B3LYP/6-31+G*.

Species	C	B	N
C ₂₄	(-0.015) – (+0.015)	–	–
C ₁₂ B ₆ N ₆	(-0.344) – (+0.201)	(+0.952) – (+1.242)	(-0.679) – (-1.206)
B ₆ N ₆ C ₁₂	(-0.454) – (+0.375)	(+1.066) – (+1.170)	(-0.942) – (-1.161)
B ₁₂ N ₁₂	–	+1.157	-1.157

with the bond length of C-B (1.587 Å) and C-N (1.451 Å).

Hydrogen storage in C₂₄ and its derivatives through NBO atomic charges

It based on Froudakis's findings on hydrogen absorption in nanotubes, point charges upon the material's surface can improve the storage capacity because they increase the binding energy of hydrogen [23]. It was shown that silicon nanotubes with alternative Si and C atoms were full of point charges [24, 25] and hence they would serve as good candidates for hydrogen storage [26].

The same phenomenon is expected for our heterofullerenes. According to calculated NBO atomic charges, the positive charges on B atoms of C₁₂B₆N₆ ranges from +0.952 to +1.242 while the negative charges on N atoms range from -0.679 to -1.206 and the positive charges on B atoms of B₆N₆C₁₂ are +1.066 to +0.170 while the negative charges on N atoms are -0.942 to -1.161. The positive charges on B atoms of B₁₂N₁₂ are +1.157 while the negative charges on N atoms are -1.157 (Compare with the range of -0.015 to +0.015 for C₂₄) (Table 3). These high point charges are predicted to establish an overall charge transfer on the surface of

heterofullerene. It seems our stable C₁₂B₆N₆ following by B₆N₆C₁₂ and B₁₂N₁₂ heterofullerene deserves more consideration in the field of hydrogen storage.

¹³C NMR characterization

The results of our calculations, as shown in Fig. 2, predict that ¹³C NMR of C₂₄ fullerene consists of two lines with chemical shielding of about 11 ppm (related to belt atoms) and 65 ppm (associated with hexagon atoms). Doped models show several lines at different positions relative to lines for C₂₄ fullerene. In NMR spectroscopy, a standard system is chosen as a reference, thus the chemical shift δ_{iso} is taken as the shielding difference between the atom of interest and the corresponding atom in the reference system. In this respect, the chemical shifts are calculated simply as the difference between the shielding of the carbon atom in the C₁₂B₆N₆ and the shielding of the corresponding carbon atom in C₂₄ fullerene. Boron, nitrogen, and carbon adopt different roles around carbon sites. The computed nuclear magnetic resonance spectrum of the B₁₂N₁₂ consists of two single peaks, confirming its *T_h* symmetry.

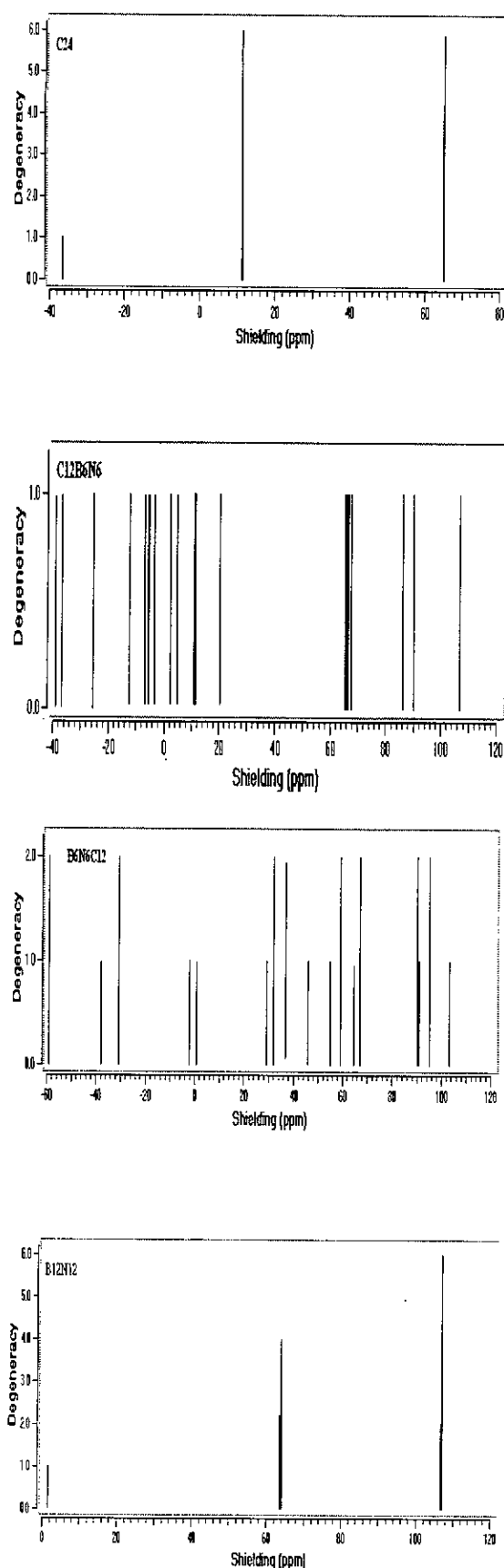


Fig. 2. ^{13}C NMR patterns.

NICS Characterization

Endohedral ^3He NMR chemical shifts have proven to be a useful tool for characterizing fullerenes and their derivatives [27]. The Nucleus-independent chemical shift (NICS) values, as a magnetic index of aromaticity, is proposed in 1996 by Schleyer and co-workers [28], at the cage center serve as predictions for the corresponding endohedral ^3He NMR chemical shifts.

C_{24} fullerene has considerably large positive value (+37) and the substitution of six CC units by BN ones results in negative NICS values at the cage center of the considered $\text{C}_{12}\text{B}_6\text{N}_6$ nanocages (Table 2). Despite the fact that electrons in the BN unit are mainly localized on nitrogen and expected to trigger nonaromaticity in these structures, all BN heterofullerenes are more aromatic than the reference molecule, C_{24} cage. As known, C_{24} contains 2 diatropic hexagons and 12 paratropic pentagons, hence corresponding ring currents combine to produce a positively large NICS (+37) at the cage center. Indeed, substitution of six CC units by BN diminishes anti-aromaticity and aromaticity in pentagonal rings and in hexagonal rings, respectively, versus C_{24} . Thus, compensation between diatropic and paratropic ring currents lead to more negative NICS values in BN-substituted heterofullerenes than those of C_{24} .

HOMO-LUMO gaps of heterofullerenes

The electrons donated by a molecule in a reaction should be from its HOMO, while the electrons captured by the molecule should locate on its LUMO. Furthermore, the atom on which the HOMO mainly distributes should have the ability for detaching electrons, whereas the atom with the occupation of the LUMO should gain electrons [29]. On this basis, the HOMO-LUMO gap is traditionally associated with chemical stability against electronic excitation, with larger gap corresponding to greater stability. On the other hand, the

conductivity of molecules is related to the HOMO-LUMO energy gaps, with smaller gap accords to more conductive species. The HOMO - LUMO gap of heterofullerene is varied depending on the type and number of doped atoms. The gap of semiconductor C_{24} is calculated to be 1.80 eV (Tab. 4).

Table 4. HOMO and LUMO energies, and HOMO-LUMO energy gaps (Gap) at B3LYP/6-31+G*

Species	HOMO (a.u.)	LUMO (a.u.)	Gap (eV)
C_{24}	-0.22364	-0.15802	1.78
$C_{12}B_6N_6$	-0.22948	-0.11183	3.20
$B_6N_6C_{12}$	-0.22794	-0.11450	3.09
$B_{12}N_{12}$	-0.29222	-0.04558	6.71

B and N doping increase the gap leading to the enhanced stability against electronic excitations. Specifically, $B_{12}N_{12}$ show significant stabilities with HOMO-LUMO gaps of 6.71 eV. It suggests that the $B_{12}N_{12}$ is insulator material but the others are semiconductors.

CONCLUSION

A DFT theoretical description has been performed to understand the effects of

atomic arrangements of dopant atoms on electronic features of the most stable cluster structures of $(BC_2N)_6$ including both C_{24} fullerene doped with six BN units and $B_{12}N_{12}$ nanocage doped with six CC units, which might be a useful guidance for the experimental studies of these nanoclusters. Our study reveals a relation between local structures within the molecules and ^{13}C NMR signals.

The electrical property analysis showed that the relative magnitude of the HOMO-LUMO gap (eV/atom) is as follows:

$$B_{12}N_{12} > C_{12}B_6N_6 > B_6N_6C_{12} > C_{24}$$

Finally NICS values are calculated at the cage center of C_{24} fullerenes and its derivatives. Compensation between diatropic and paratropic ring currents cause an enhancement in aromaticity of all considered $C_{12}B_6N_6$ nanocages with negative NICS at the cage center (from -0.67 to -11) versus C_{24} (+37). The predicted NICS values may be useful for the identification of the heterofullerenes through their endohedral 3He NMR chemical shifts.

REFERENCES

- [1] (a) L. Türker, Journal of Molecular Structure: THEOCHEM 593 (2002) 149. (b) L. Türker, Journal of Molecular Structure: THEOCHEM 624 (2003) 233.
- [2] H.W. Kroto, J.R. Heath, S.C. O'Brien, R.F. Curl, R.E. Smalley, Nature 318 (1985) 162.
- [3] D.A. Bochvar, E.G. Gal'perm, Proc. Acad. Sci. USSR 209 (1973) 239.
- [4] J. Pattanayak, T. Kar, S. Scheiner, J. Phys. Chem. A 108 (2004) 7681.
- [5] Z. Chen, K. Ma, Y. Pan, J. Mol. Struct. (THEOCHEM), 490 (1999) 61.
- [6] Z. Chen, K. Ma, H. Zhao, J. Mol. Struct. (THEOCHEM) 466 (1999) 127.
- [7] (a) Pokropivny, V. V.; Pokropivny, A. V.; Skorokhod, V. V.; Kurdyumov, A. V. Dopov. Nats. Akad. Nauk Ukr. 1999, 4, 112. (b) Pokropivny, V. V.; Pokropivny, A. V. Phys. Solid State 2004, 46, 392. (c) Pokropivny, V. V.; Skorokhod, V. V.; Oleinik, G. S.; Kurdyumov, A. V.; Bartnitskaya, T. S.; Pokropivny, A. V.; Sisonyuk, A. G.; Sheichenko, D. M. J. Solid State Chem. 2000, 154, 214.
- [8] A. D. Becke, Phys. Rev. A 38 (1988) 3098.
- [9] A. D. Becke, J. Chem. Phys. 98 (1993) 5648.
- [10] C. Lee, W. Yang, R.G. Parr, Phys. Rev. B 37 (1988) 785.
- [11] M.J. Frisch, G.W. Trucks, H.B. Schlegel, G.E. Scuseria, M.A. Robb, J.R. Cheeseman, V.G. Zakrzewski, J.A. Montgomery Jr., R.E. Stratmann, J.C. Burant, S. Dapprich, J.M. Millam, A.D.

- Daniels, K.N. Kudin, M.C. Strain, O. Farkas, J. Tomasi, V. Barone, M. Cossi, R. Cammi, B. Mennucci, C. Pomelli, C. Adamo, S. Clifford, J. Ochterski, G.A. Petersson, P.Y. Ayala, Q. Cui, K. Morokuma, D.K. Malick, A.D. Rabuck, K. Raghavachari, J.B. Foresman, J. Cioslowski, J.V. Ortiz, A.G. Baboul, B.B. Stefanov, G. Liu, A. Liashenko, P. Piskorz, I. Komaromi, R. Gomperts, R.L. Martin, D.J. Fox, T. Keith, M.A. Al-Laham, C.Y. Peng, A. Nanayakkara, C. Gonzalez, M. Challacombe, P.M.W. Gill, B. Johnson, W. Chen, M.W. Wong, J.L. Andres, C. Gonzalez, M. Head-Gordon, E.S. Replogle, J.A. Pople, *Gaussian*, 98, Gaussian, Inc., Pittsburgh, PA, (1998).
- [12] P.C. Hariharan, J.A. Pople, *Mol. Phys.* 27 (1974) 209.
- [13] M.M. Francl, W.J. Pietro, W.J. Hehre, J.S. Binkley, M.S. Gordon, D.J. DeFrees, J.A. Pople, *J. Chem. Phys.* 77 (1982) 3654.
- [14] T. Clark, J. Chandrasekhar, G.W. Spitznagel, P.v.R. Schleyer, *J. Comput. Chem.* 4 (1983) 294.
- [15] M.J. Frisch, J.A. Pople, J.S. Binkley, *J. Chem. Phys.* 80 (1984) 3265.
- [16] R. Ditchfield, W.J. Hehre, J.A. Pople, *J. Chem. Phys.* 54 (1972) 724.
- [17] R.S. Drago, Saunders College Publishing, Florida, (1992).
- [18] C.J. Jameson, in: G.A. Webb (Ed.), *Specialized Periodical Reports on NMR*, vols. 10–21, Royal Society of Chemistry, London, 1981.
- [19] A.E. Reed, L.A. Curtiss, F. Weinhold, *Chem Rev* 88 (1988) 899.
- [20] Jensen, F.; Koch, H. *J. Chem. Phys.* 108, (1998), 3213.
- [21] Fokin, A. A.; Jiao, H.; Schleyer, P. v. R. *J. Am. Chem. Soc.* 120, (1998), 9364–9365.
- [22] Chen, Z.; Jiao, H.; Bühl, M.; Hirsch, A.; Thiel, W. *Theor. Chem. Acc.* 106, (2001), 352.
- [23] G.E. Froudakis, *Nano Lett.* 1 (2001) 531.
- [24] A. Mavrandonakis, G.E. Froudakis, M. Schnell, M. Muhlhauser, *Nano Lett.* 3 (2003) 1481.
- [25] M. Menon, E. Richter, A. Mavrandonakis, G. Froudakis, A.N. Andriotis, *Phys. Rev. B* 69 (2004) 115322.
- [26] G. Mpourmpakis, G.E. Froudakis, G.P. Lithoxoos, J. Samios, *Nano Lett.* 6 (2006) 1581.
- [27] M. Saunders, R.J. Cross, H.A. Jimenez-Vazquez, R. Schimshi, A. Khong, *Science* 271 (1996) 1693.
- [28] P.V.R. Schleyer, C. Maerker, A. Dransfeld, H. Jiao, N.J.R.V.E. Hommes, *J. Am. Chem. Soc.* 118 (1996) 6317.
- [29] C. Tang, W. Zhu, K. Deng, *Journal of Molecular Structure: Theochem* 909 (2009) 43.

